102413

Available online at www.sciencedirect.com
ScienceDirect
Chemical Geology 249 (2008) 294–306
CHEMICAL GEOLOGY
INCLUDING ISOTOPE GEOSCIENCE
www.elsevier.com/locate/chemgeo

The stable Cr isotope inventory of solid Earth reservoirs determined by double spike MC-ICP-MS

R. Schoenberg *, S. Zink, M. Staubwasser, F. von Blanckenburg

Institute for Mineralogy, University of Hannover, Callinstrasse 3, D-30167 Hannover, Germany

Received 9 August 2007; received in revised form 30 January 2008; accepted 31 January 2008

Edited by: B. Bourdon

Abstract

We present the first comprehensive set of stable Cr isotope data for the major igneous silicate Earth reservoirs, Cr(III)-rich ores and minerals, and hydrothermal chromates. These were determined by MC-ICP-MS using a double spike technique. Mantle xenoliths, ultramafic rocks, cumulates, as well as oceanic and continental basalts share a common Cr isotope composition with an average $\delta^{53/52}$Cr value of −0.124±0.101‰ (2 SD) relative to the isotopically certified chromium standard NIST SRM 979. An isotopic difference between mantle xenoliths and basalts, as was reported for iron, was not observed for chromium. Thus, the change in oxidation state that is observed when solid mantle rocks, containing only trivalent chromium, partially melt to form basaltic melts, which predominantly contain bivalent chromium, does not cause any measurable Cr isotope fractionation. Chromite separates from major chromitite seams of the Bushveld and Great Dyke layered igneous complexes are invariable in their Cr isotope compositions and reproduce within uncertainties the average $\delta^{53/52}Cr_{SRM\ 979}$ value of igneous silicate Earth reservoirs. This is important for environmental stable Cr isotope studies, because it labels the approximate isotope composition of industrial Cr(VI) pollutants. The Cr isotope compositions of hydrothermal lead chromates (crocoites $PbCr^{VI}O_4$) from various localities yield $\delta^{53/52}Cr_{SRM\ 979}$ values between 0.640 and 1.037‰; these Cr isotope compositions are substantially heavier than those of igneous silicate rocks from which the chromium was leached. Precipitation experiments revealed an isotope fractionation of $\Delta^{53/52}Cr_{(crocoite-Cr(VI)aq)}$ of only ca. +0.10±0.05‰ at a temperature of 20 °C. Thus, the heavy Cr isotope signature of crocoites is most likely the result of repeated redox cycling of chromium in hydrothermal processes.
© 2008 Elsevier B.V. All rights reserved.

Keywords: Stable chromium isotope; Silicate Earth; Crocoite; Chromate; Chromium fractionation

1. Introduction

Published experiments have revealed that the reduction of Cr (VI) to Cr(III) in aqueous solutions is accompanied by a significant mass-dependent Cr isotope fractionation of −3.4‰ on the $^{53}Cr/^{52}Cr$ ratio (Ellis et al., 2002). Adsorption of Cr(VI) onto γ-Al_2O_3 and goethite may cause substantial initial kinetic isotope fractionation (0.70‰ on the $^{53}Cr/^{52}Cr$ ratio for exposures of <2 h), but equilibrium is reached within less than 24 h and equilibrium isotope fractionation is insignificant (≪0.04‰ on $^{53}Cr/^{52}Cr$; Ellis et al., 2004). These properties make stable Cr isotope systematics a potential tracer to detect and quantify redox changes in a variety of geochemical reservoirs. For example measurements of stable Cr isotopes in groundwater allow to trace toxic Cr(VI) pollution of aquifers — be it through anthropogenic contamination or through natural dissolution and oxidation of Cr(III) from ultramafic rock bodies. In addition, the natural attenuation of Cr(VI) by reduction to the environmentally much less harmful Cr(III) can be quantified (Blowes, 2002). A prerequisite to utilization of stable Cr isotope fingerprints as process tracers of the global chromium cycle is knowledge of the Cr isotope composition of typical silicate Earth reservoirs. This igneous rock baseline provides the starting point of the global chromium cycle that involves

* Corresponding author. Tel.: +49 511 762 5998; fax: +49 511 762 2110.
E-mail address: r.schoenberg@mineralogie.uni-hannover.de
(R. Schoenberg).

0009-2541/$ - see front matter © 2008 Elsevier B.V. All rights reserved.
doi:10.1016/j.chemgeo.2008.01.009

31128

weathering of igneous and sedimentary rocks, the riverine transport of chromium as dissolved and solid matter and eventually the deposition in the marine environment. However, with the exception of the Cr isotope compositions of three basaltic standard reference rocks (Ellis et al., 2002) such data is not yet available.

Here, the first comprehensive characterization of the stable Cr isotope composition of silicate rocks from the Earth's mantle and crust is presented. High-temperature Cr isotope fractionation during partial mantle melting was investigated by determining the Cr isotope compositions of mantle xenoliths and basaltic rocks. A first assessment of possible fractionation of Cr isotopes through metamorphism was attempted by measuring Cr-bearing metamorphic silicates (i.e. uvarovite and fuchsite) from different geological settings. Knowledge of the Cr isotope composition of technical chromium, that is used for metal plating, leather tanning, and timber preservation, is important for environmental studies concerning Cr(VI) pollution by the wastes of these industries. For this purpose, the Cr isotope composition of chromite ores from two major chromium sources, the Bushveld Complex, South Africa, and the Great Dyke, Zimbabwe, were measured. Furthermore, possible Cr isotope fractionation under oxidizing conditions in near-surface continental hydrothermal systems was investigated by measuring the Cr isotope composition of crocoites from Beresovsk and Yekaterinburg, Russia, and Calenberg, Germany. Finally, a first set of marine sediment data from the Arabian Sea is presented.

2. Analytical procedures

2.1. Cr separation from solid materials

Typically 100 mg of the silicate samples were digested in HF:HNO_3 mixtures in closed PFA vials on a hot plate at 150 °C. After drying down, the residues were taken up in aqua regia and reheated to 170 °C for several hours to destroy fluoride complexes that may have formed during the digestion. Replicates of silicate rocks, in particular mantle xenoliths, were digested in HF:HNO_3 mixtures by microwave agitation at 200 °C. After drying down the residues were taken up in aqua regia and full digestion of fluoride complexes and possible undissolved spinel phases was ensured by renewed heating to 200 °C in the microwave oven. After digestion of the silicate minerals in bulk marine sediments using HF:HNO_3 mixtures, significant amounts of organic compounds remained undissolved. These were taken up in small volumes of perchloric acid, heated to 160 °C for several hours and taken to dryness. Perchloric acid addition, heating and drying down was repeated until all organic compounds were dissolved. Chromite samples were digested by microwave agitation in aqua regia at 200 °C. Upon full digestion of the samples, small aliquots were removed, dried down and taken up in 0.3 mol L^{-1} HNO_3 to determine the samples' elemental compositions by inductively coupled plasma optical emission spectroscopy (ICP-OES) on a Varian Vista Pro instrument. The remaining solutions were then taken to dryness and dissolved in 2 mol L^{-1} nitric acid to which an adequate amount of the ^{50}Cr–^{54}Cr double spike was added. Our ^{50}Cr–^{54}Cr double spike is in the Cr(III) form and stored in 2 mol L^{-1} nitric acid, because this matrix keeps chromium in the reduced trivalent state (see below). In nitric acid spike and sample were easily homogenized by heating the solutions in closed vials. Tests showed that addition of the spike before sample digestion is not necessary, since no chromium is lost during the sample dissolution by acid attack. Finally, all solutions were dried down again and the residues taken up in dilute hydrochloric acid for the Cr extraction.

We employed an anion exchange chromatography technique adapted from previously published methods (Ball and Bassett, 2000; Frei and Rosing, 2005) to separate chromium of natural samples from the other matrix elements. In contrast to the original method described by Ball and Bassett (Ball and Bassett, 2000) and in accord with that of Frei and Rosing (Frei and Rosing, 2005) we had to perform this chromium separation from rock matrices in dilute hydrochloric acid instead of (near) pH-neutral solutions, to avoid precipitation of the matrix elements. This separation method is based on the exchange of chloride ions on the active surface of the Dowex AG 1X8 anion resin by the Cr(VI)-oxyanions. Most other elements form cationic or neutral complexes in dilute hydrochloric acid that are not adsorbed by the resin. However, after sample digestion and uptake in dilute hydrochloric acid all Cr is present as Cr(III). Therefore, before anion exchange separation is carried out, oxidation of Cr(III) to Cr(VI) is achieved using $(NH_4)_2S_2O_8$ as oxidizing agent (Götz and Heumann, 1988). For this purpose the sample-spike mixture is dissolved in 0.25 mL 1 mol L^{-1} HCl and diluted with 8.75 mL ultrapure H_2O and transferred to a 25 mL Erlenmeyer flask. 1 mL 0.2 mol L^{-1} $(NH_4)_2$ S_2O_8 is added to the Erlenmeyer flask to yield a total solution of 0.025 mol L^{-1} HCl and 0.02 mol L^{-1} $(NH_4)_2$ S_2O. The Erlenmeyer flask is covered with a watch glass and placed on a hot plate at 120–130 °C for 2 h to oxidize Cr(III) to Cr(VI). In the meantime, a Spectrum® PP Column 104704 is filled with 2 mL of Dowex AG 1X8, 100–200 mesh, anion exchange resin. The resin is first sequentially cleaned with 5 mL of 5 mol L^{-1} HNO_3, ultrapure H_2O, 0.2 mol L^{-1} HCl, and ultrapure H_2O again and then pre-conditioned with 5 mL 0.025 mol L^{-1} HCl. After cooling to room temperature, the oxidized sample in the Erlenmeyer flask is directly loaded onto the anion exchange column. The matrix of the sample is eluted with a total of 20 mL 0.2 mol L^{-1} HCl, followed by 16 mL of ultrapure H_2O. A clean 11 mL PFA beaker is placed under the column. Addition of 1 mL 2 mol L^{-1} HNO_3 to the resin reduces Cr(VI) to Cr(III) (Götz and Heumann, 1988; Ball and Bassett, 2000). After waiting for 2 h to allow the reduction to take place, the sample Cr is released from the resin by sequential addition of another 9 mL 2 mol L^{-1} HNO_3. When necessary, further cleaning of the chromium separates from vanadium and titanium was achieved by the liquid extraction method of Remya and Reddy (Remya and Reddy, 2004) using the trialkylphosphine oxide Cyanex® 923 (Cytec Industries Inc.). The separation yields for chromium are 70 to 85% for the combined anion exchange and liquid–liquid extraction methods and 80 to 90% if only anion exchange purification is required. Total procedure blanks are less than 20 ng for the combined separation method, which is negligible

compared to the amount of chromium separated from the rocks and minerals studied here.

2.2. Cr isotope measurements

So far, precise radiogenic isotope ratio measurements of chromium by thermal ionization mass spectrometry (TIMS) allowed to determine the radiogenic in-growth of ^{53}Cr through the decay of the short-lived nuclide ^{53}Mn (half-life of 3.7 Ma) in meteoritic materials. In this approach, the instrumental mass bias caused by the thermal vaporization of the sample in the mass spectrometer can be determined and corrected using the natural $^{50}Cr/^{52}Cr$ ratio and an exponential law (Lugmair and Shukolyukov, 1998). However, accurate and reliable determination of the stable, mass-dependent chromium isotope fractionation of natural samples by TIMS was compromised by mass-dependent isotope fractionation of chromium that may occur during its chemical purification (Ball and Bassett, 2000; Ellis et al., 2002), and the sometimes unpredictable drift of instrumental mass bias (Ball and Bassett, 2000). The addition of a ^{50}Cr–^{54}Cr double spike of known isotope composition to a sample before chemical purification allowed accurate correction of both, the chemical and the instrumental shifts in Cr isotope abundances (Ellis et al., 2002). With this method a 2σ external reproducibility of ±0.2‰ on the $^{53}Cr/^{52}Cr$ ratio was achieved, which is somewhat inferior to recently reported external reproducibilities of ±0.05 to 0.1‰ for stable transition metal isotope ratio determinations by MC-ICP-MS (e.g. Johnson et al., 2004).

In this study we investigated the accuracy and precision obtained by ^{50}Cr–^{54}Cr double spike Cr isotope ratio determinations carried out by MC-ICP-MS analyses. Our double spike correction returns Cr isotope compositions of samples as the per mil difference to the isotope composition of the NIST SRM 3112a Cr standard. We used this standard for our spike-calibration and the accuracy and reproducibility tests [Eq. (1)]. However, to maintain inter-laboratory comparability of Cr isotope data we recalculate our data of natural samples relative to the certified Cr isotope standard NIST SRM 979 that was used in previous works (Ball and Bassett, 2000; Ellis et al., 2002, 2004):

$$[\text{sample}]\delta^{53/52}\text{Cr}_{(\text{SRM979})} = \left[\left(\frac{(^{53}\text{Cr}/^{52}\text{Cr})\ \text{of sample}}{(^{53}\text{Cr}/^{52}\text{Cr})\ \text{of SRM979}}\right) - 1\right] \times 1000 \quad (1)$$

All Cr isotope measurements were performed on a ThermoFinnigan Neptune MC-ICP mass spectrometer equipped with nine Faraday collectors that allow for simultaneous collection of all four chromium beams ($^{50}Cr^+$, $^{52}Cr^+$, $^{53}Cr^+$, $^{54}Cr^+$) together with $^{48}Ti^+$, $^{51}V^+$, and $^{56}Fe^+$ as monitors for small interferences of ^{50}Ti and ^{50}V on ^{50}Cr and ^{54}Fe on ^{54}Cr, respectively. For Cr isotope measurements the instrument is always operated in high-resolution mode with a mass resolution R of ca. 9000 to 12,000 (for the definition of R see Weyer and Schwieters, 2003) to physically separate $^{40}Ar^{12}C$ from ^{52}Cr, $^{40}Ar^{14}N$ from ^{54}Cr and $^{40}Ar^{16}O$ from ^{56}Fe. Chromium separates were taken up in 0.1 mol L^{-1} HNO_3 to yield solutions with a Cr concentration of 2 μg mL^{-1}. The samples were nebulized by a Teflon micro-nebulizer in free aspiration mode with an uptake rate of ~40 μL min^{-1} and the aerosol was sprayed into the plasma via the ThermoFinnigan stable introduction system (SIS). Under these sample uptake conditions typical ion beams of 8×10^{-11} A were obtained on $^{52}Cr^+$.

A ^{50}Cr–^{54}Cr double spike of well-known isotope composition was added to all samples and standard solutions before chemical treatment. The double spike addition allows correcting a possible artificial fractionation of Cr isotopes that may be caused by the separation of chromium from the sample matrix, especially during the anion exchange chromatography, as was for example observed for Fe isotopes (Anbar et al., 2000). A large fractionation of the Cr isotopes may be caused by incomplete reduction of Cr(VI) to Cr(III) (Ellis et al., 2002) that is necessary to release the purified chromium from the anion exchange resin. The extent of Cr isotope fractionation by incomplete reduction of Cr(VI) to Cr(III) during the ion exchange purification was tested and is described in detail in Section 2.5. Furthermore, the addition of the double spike to samples and standards enables an accurate in-run correction of the instrumental mass bias (e.g. Johnson and Beard, 1999; Siebert et al., 2001; Ellis et al., 2002; Dideriksen et al., 2006). Another advantage of the in-run correction of the instrumental mass bias by the double spike method is the instant correction of the mass bias drift during every measured cycle. The standard-sample-bracketing method, the most commonly used technique to correct the instrumental mass bias of stable isotope ratio measurements by MC-ICP-MS, assumes linear mass bias drift over the time interval of one set of standard-sample-standard measurements. However, such a set of measurements takes several minutes to perform, during which the mass bias drift is not necessarily linear (see e.g. Schoenberg and von Blanckenburg, 2005). Our double spike correction method is based on the iterative solution reported by Compston and Oversby (1969), with the adaption to the exponential instead of the linear fractionation law (Albarede et al., 2004). The correction is employed to every single measurement cycle allowing for direct statistical treatment of individual mass spectrometric runs. Other double spike correction methods (Siebert et al., 2001) have been tested and gave identical results. A double spike correction for a four isotope element returns three values: (1) the instrumental fractionation factor (mass bias) per atomic mass unit, (2) the natural fractionation factor of the sample per atomic mass unit that then can be used to recalculate absolute isotope ratios of the sample and the respective δ-values, and (3) the exact spike-to-sample ratio that allows a highly accurate determination of the samples' Cr concentrations (i.e. the isotope dilution method).

The baseline correction was performed by averaging background intensities of the pure carrier solution (i.e. 0.1 mol L^{-1} HNO_3) that were measured on-peak before and after every sample analysis. Background measurements consisted of 45 and sample measurements of 90 cycles, respectively. Signals for each measurement cycle were integrated during 4 s. A sample washout time of 3 min guaranteed that signals returned to

background levels. A standard solution of known isotope composition (e.g. NIST SRM 979) was measured every five samples.

2.3. Accuracy and reproducibility of double spike MC-ICP-MS measurements

2.3.1. Reference standard materials

The long-term instrumental reproducibility was determined by measuring the NIST SRM 3112a Cr standard ($N=107$) against itself over the time period between January 2005 and November 2006. For each measurement session an adequate amount of the ^{50}Cr–^{54}Cr double spike was homogenized with an aliquot of our NIST SRM 3112a stock solution and subject to the Cr separation method lined out in Section 2.1. A compilation of these data subdivided into the daily measurement sessions is given in Fig. 1a. The average $\delta^{53/52}Cr_{SRM\ 3112a}$ value of all NIST SRM 3112a standard measurements is -0.012 ± 0.043‰ (2 SD). However, the internal variability in $\delta^{53/52}Cr_{SRM\ 3112a}$ of the daily measurement sessions appears to be more precise than the long-term reproducibility of 0.043‰. When internally normalizing the average $\delta^{53/52}Cr_{SRM\ 3112a}$ value of each daily measurement session to the nominal $\delta^{53/52}Cr_{SRM\ 3112a}$ value of zero, the long-term instrumental reproducibility decreases to 0.024‰ (2 SD; Fig. 1b). Such offsets of session averages to the nominal value, although to a much larger extent (i.e. by ±0.2‰ in $\delta^{56}Fe/^{54}Fe$ values), have already been described for double spike Fe isotope data (Dideriksen et al., 2006). We assume an exponential instrumental mass bias in our double spike correction method, since Fe isotope data measured on our instrument plot along a near exponential slope in $\ln(^{57}Fe/^{54}Fe)$ versus $\ln(^{56}Fe/^{54}Fe)$ space (Schoenberg and von Blanckenburg, 2005). The true instrumental mass bias, however, might deviate from the exponential law and thus cause such offsets in $\delta^{53/52}Cr$ values from measurement session to measurement session. Therefore, the Cr isotope compositions of natural samples of a measurement session are corrected for this offset.

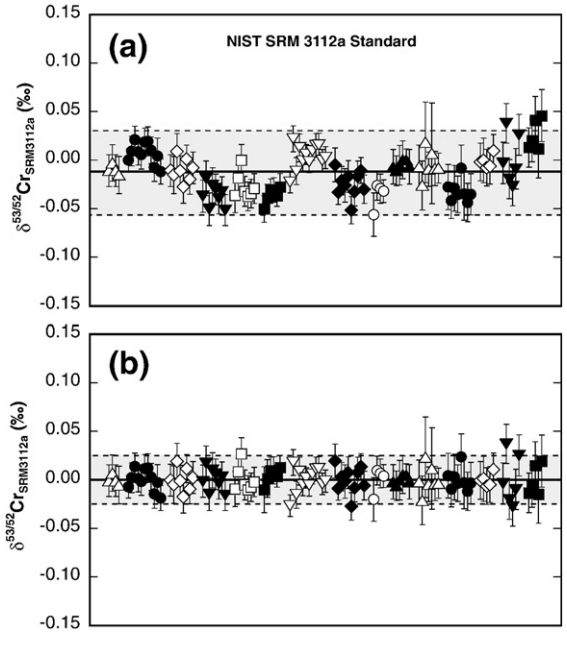

Fig. 1. Long-term reproducibility of $\delta^{53/52}Cr_{SRM\ 3112a}$ values for the NIST SRM 3112a chromium standard. Individual analytical sessions are characterized by different symbols. Panel (a) shows data that were uncorrected and panel (b) the same data that were corrected for small variations of the average $\delta^{53/52}Cr_{SRM\ 3112a}$ values between the different analytical sessions. Uncertainties are the internal 2 standard errors of the single measurements. The gray areas give the 2 standard deviation envelope for the average $\delta^{53/52}Cr_{SRM\ 3112a}$ value.

2.3.2. Natural samples

Often the external reproducibility of isotope ratio measurements of natural samples is inferior to that of pure isotope standards, due to sample heterogeneity and small impurities after chemical extraction of the target element. Indeed, the external reproducibility for all the replicates of natural samples ($N=54$) is 0.048‰ on $\delta^{53/52}Cr$, which compares to 0.024‰ for NIST SRM 3112a.

Regardless of the analytical reproducibility, sample isotope ratios can be affected by a bias that arises from the choice of mathematical law to describe the natural isotope fractionation used in the double spike algorithm. Our algorithm assumes an exponential law for the natural isotope fractionation. This assumption is valid for kinetic, but not for equilibrium isotope fractionation, as these two modes of fractionation follow different laws (e.g. Young et al., 2002). For chromium, isotope fractionation factors α between two samples or two different conditions a and b can be described as:

$$\alpha_{(^{53}Cr/^{52}Cr)}=\frac{\left(^{53}Cr/^{52}Cr\right)_a}{\left(^{53}Cr/^{52}Cr\right)_b}\quad\text{or}\quad\alpha_{(^{54}Cr/^{52}Cr)}=\frac{\left(^{54}Cr/^{52}Cr\right)_a}{\left(^{54}Cr/^{52}Cr\right)_b}\qquad(2)$$

In mass-dependent isotope fractionation these two fractionation factors follow the relation:

$$\alpha\left(^{53}Cr/^{52}Cr\right)=\alpha\left(^{53}Cr/^{52}Cr\right)^{\beta}\qquad(3)$$

The exponent β is different for equilibrium and kinetic isotope fractionation:

$$\beta_{equilibrium}=\frac{\left[\frac{1}{M_{53}}-\frac{1}{M_{52}}\right]}{\left[\frac{1}{M_{54}}-\frac{1}{M_{52}}\right]}=0.5099\quad\text{and}$$

$$\beta_{kinetic}=\beta_{exponential}=\frac{\ln\left[\frac{M_{53}}{M_{52}}\right]}{\ln\left[\frac{M_{54}}{M_{52}}\right]}=0.5052\qquad(4)$$

where M_{52}, M_{53}, and M_{54} describe the exact atomic masses of ^{52}Cr, ^{53}Cr, and ^{54}Cr (De Laeter et al., 2003), respectively. This means that in $\delta^{53/52}Cr$ versus $\delta^{54/52}Cr$ space the equilibrium fractionation vector has a slope of 0.5099, while the kinetic or exponential fractionation vector has a slope of 0.5052. Thus, with our double spike method the inaccuracy in the Cr isotope composition of a sample that underwent equilibrium isotope fractionation is −0.009‰ per 1‰ on the true $\delta^{53/52}Cr$ value. If it were known whether the Cr isotopes of a sample fractionated under equilibrium conditions, then the algorithms of our double

spike correction method could be adjusted accordingly. However, usually such information is not available. Therefore, the uncertainty on the accuracy of double spike measurements arising from the mode of isotope fractionation of the natural samples has to be accounted for in the propagation of the measurements' uncertainties. For natural samples we therefore calculate the uncertainty on the $\delta^{53/52}$Cr value of a single measurement as the error propagation of the possible inaccuracy resulting from the double spike correction and the external reproducibility of natural samples:

$$2SD = \sqrt{\left(-0.009‰ * \delta^{53/52}Cr_{sample}\right)^2 + \left(2\sigma_{external}\right)^2} \quad (5)$$

where $2\sigma_{external}$ gives the external reproducibility in $\delta^{53/52}$Cr for natural samples, which in our case is 0.048‰. While the uncertainty of 0.049‰ for a sample with a $\delta^{53/52}$Cr value of 1‰, calculated according to Eq. (5), only marginally exceeds the external reproducibility of natural samples, it becomes significant for samples with $\delta^{53/52}$Cr values of several ‰, such as measured in contaminated groundwaters (Ball and Bassett, 2000; Ellis et al., 2002). Samples with $\delta^{53/52}$Cr values of 4‰ and 7‰, for example, have propagated uncertainties of 0.060‰ and 0.079‰ respectively. For replicate analyses of a sample we either report this propagated uncertainty using the sample's average $\delta^{53/52}$Cr value or we give the 2 standard deviation of the replicated $\delta^{53/52}$Cr values, whichever is larger.

The effect of the amount of the double spike added to a sample on the accuracy of the samples' $\delta^{53/52}$Cr value was tested by doping aliquots of the NIST SRM 3112a standard with different amounts of the double spike ($conc._{spike}/conc._{NIST\ SRM\ 3112a}$=0.05–2.00). Fig. 2 reveals that the accuracy of $\delta^{53/52}Cr_{SRM\ 3112a}$ values is relatively insensitive to the amount of double spike that is added to the NIST SRM 3112a standard. Only at $conc._{spike}/conc._{NIST\ SRM\ 3112a}$ ratios smaller than 0.2 the $\delta^{53/52}$Cr values of the NIST SRM 3112a standard appeared to tend towards inaccurate values. Based on these results, the amount of double spike added to natural samples is always aimed to yield $conc._{spike}/conc._{sample}$ ratios between 0.25 and 0.40.

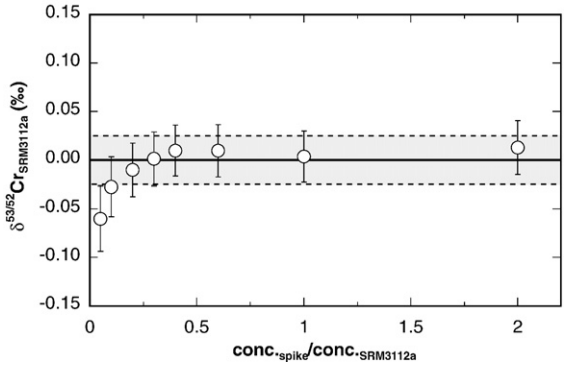

Fig. 2. Accuracy of $\delta^{53/52}Cr_{SRM\ 3112a}$ values as function of the amount of double spike added to the NIST SRM 3112a chromium standard. The shaded area gives the 2 standard deviation envelope of the external reproducibility for standard measurements with our double spike method (see Fig. 1b).

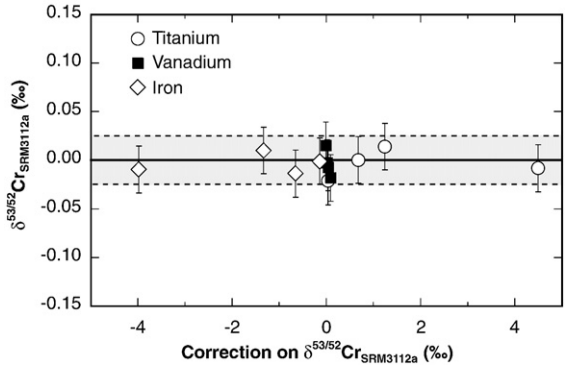

Fig. 3. Test for the accuracy of the interference corrections of ^{50}Ti, ^{50}V on ^{50}Cr and ^{54}Fe on ^{54}Cr. Amount of interferences on the monitor isotopes ^{48}Ti, ^{51}V, and ^{56}Fe were 0.01, 0.05, 0.10, and 0.30 volts and signal intensities on ^{52}Cr were ca. 7 volts ($R=10^{11}$ Ω).

The accuracy of the interference correction of ^{50}Ti and ^{50}V on ^{50}Cr and ^{54}Fe on ^{54}Cr, respectively, was tested by doping different amounts of Ti, V, or Fe to spiked aliquots of the NIST SRM 3112a Cr standard. Fig. 3 shows that within uncertainties all interference-corrected $\delta^{53/52}Cr_{SRM\ 3112a}$ values of the Ti, V, and Fe doped standards plot within the 2σ envelope of the instrumental reproducibility of ±0.024‰. It must be noted, however, that in these test runs the highest signals on the interference monitors ^{48}Ti, ^{51}V, and ^{56}Fe were approximately 15–30 times higher than those observed in any natural samples measured so far. Our interference correction is based on an iterative solution in which the instrumental fractionation factor of Cr obtained by the double spike correction is used to artificially fractionate the natural ^{48}Ti/^{50}Ti, ^{51}V/^{50}V, and ^{56}Fe/^{54}Fe values recommended by the International Union of Pure and Applied Chemistry IUPAC (De Laeter et al., 2003). These altered ratios are then used to subtract the signals of interfering nuclides from those of chromium, which yields a new set of chromium isotope ratios and thus a new instrumental fractionation factor for Cr. It must be born in mind, however, that in a plasma source different elements fractionate to various extents (e.g. Maréchal et al., 1999; Arnold et al., 2004). Nevertheless, the data plotted in Fig. 3 demonstrate that our interference correction method yields accurate Cr isotope values, even for amounts of isobaric interferences on Cr isotopes that largely exceeded those observed during sample measurements.

2.4. Intercalibration of the NIST SRM 3112a, NIST SRM 979, and IRMM-012 Cr standards

Relative to our NIST SRM 3112a chromium standard, against which our double spike was calibrated, we determined the stable chromium isotope compositions of the certified isotope standard reference materials SRM 979 (Shields et al., 1966) of the National Institute of Standards and Technology (NIST), USA, and IRMM-012 of the Institute for Reference Materials and Measurements (IRMM), Belgium. Furthermore, the stable Cr isotope compositions of two Merck® Cr ICP standards, a 1000 mg L^{-1} $Cr(III)_{aq}$ and a 1000 mg L^{-1} $CrO_4^{2-}{}_{aq}$, were also determined. All results are reported relative to NIST SRM 979 (Table 1).

Table 1
Concentrations and Cr isotope compositions of different chromium standards

Sample	$Cr_{measured}$ [μg g^{-1}]	±	2 SD [abs.]	Cr_{given} [μg g^{-1}]	±	2 SD [abs.]	$\delta^{53/52}Cr_{SRM\ 979}$	±	2 SD [b]	N
NIST SRM 979	50928	±	255	54616	±	230	0.000	±	0.016	18
IRMM-012	52.96	±	0.26	53.04	±	0.22	0.023	±	0.013	5
NIST SRM 3112a	100.3	±	0.5	100.4	±	0.5	−0.067	±	0.024	107
Merck Cr(III) Std	978.7	±	4.9	984.2	±	3.0	−0.443	±	0.022	4
Merck Cr(VI) Std	445.3	±	2.2	448.7	±	1.3	−0.031	±	0.026	4
Partial Cr release from the anion resin				*$F_{Cr(VI)}$ left on column*						
Loaded standard	1.204 [a]	±	0.060	$F_{Cr(VI)}$	=	1.00	0.000	±	0.024	1
Fraction 1	0.2248	±	0.0011	$F_{Cr(VI)}$	=	0.81	−2.764	±	0.035	1
Fraction 2	0.1474	±	0.0007	$F_{Cr(VI)}$	=	0.69	−2.047	±	0.030	1
Fraction 3	0.1200	±	0.0006	$F_{Cr(VI)}$	=	0.59	−1.444	±	0.027	1
Fraction 4	0.3028	±	0.0015	$F_{Cr(VI)}$	=	0.34	−0.059	±	0.024	1
Fraction 5	0.2556	±	0.0013	$F_{Cr(VI)}$	=	0.13	3.666	±	0.041	1
Fraction 6	0.04348	±	0.00022	$F_{Cr(VI)}$	=	0.09	5.194	±	0.053	1

[a] Concentration determined by ICP-OES; all other concentrations were determined by isotope dilution using double spike MC-ICP-MS.
[b] Uncertainty for the standards is given as 2SD of the population to demonstrate the reproducibility. For the partial Cr release experiment uncertainties are calculated according to Eq. (5), using the external reproducibility for standards (i.e. 0.024‰) instead of natural samples.

Within uncertainties NIST SRM 979 and IRMM-012 are identical in their stable Cr isotope compositions, which is not surprising since IRMM-012 that is delivered as $Cr(III)_{aq}$ in 1 mol L^{-1} HCl has originally been produced from the NIST SRM 979 standard, which is a hydrated chromium nitrate salt ($[Cr(NO_3)_3 \times 9H_2O]$). Both these standards are heavier in their Cr isotope compositions than the NIST SRM 3112a standard; by 0.067‰ in the $^{53}Cr/^{52}Cr$ ratio for NIST SRM 979 and by 0.090‰ in the $^{53}Cr/^{52}Cr$ ratio for IRMM-012, respectively. The stable Cr isotope compositions of the two Cr ICP standards are variable too, with $\delta^{53/52}Cr_{SRM\ 979}$ values of −0.443‰ for the Cr (III) and −0.031‰ for the CrO_4^{2-} standards, respectively. The differences in the Cr isotope compositions of NIST SRM 979, NIST SRM 3112a, and the Merck® Cr(III) ICP standard were confirmed by the Illinois group on aliquots of our original standard solutions; they obtained $\delta^{53/52}Cr_{SRM\ 979} = -0.056 \pm 0.120$ ($N=20$) for the NIST SRM 3112a, and $\delta^{53/52}Cr_{SRM\ 979} = -0.390 \pm 0.100$ ($N=1$) for the Merck® Cr(III) ICP standard using their own double spike solution and measuring on a Nu Instruments MC-ICP-MS in high-resolution mode (personal communication with Thomas M. Johnson, University of Illinois at Urbana-Champaign, November 2007). Note that the difference in reproducibility of $\delta^{53/52}Cr_{SRM\ 979}$ values between the two laboratories is caused by differences in ion beam intensities, which have been higher in our approach. As mentioned before, the stable Cr isotope data of natural samples are recalculated relative to the certified Cr isotope standard NIST SRM 979 to maintain inter-laboratory comparability of Cr isotope data according to Eq. (6).

$$[\text{sample}]\delta^{53}Cr_{(SRM979)} = [\text{sample}]\delta^{53}Cr_{(SRM3112a)} - 0.067‰ \quad (6)$$

2.5. Cr isotope fractionation during anion exchange separation

A column experiment was carried out to assess the potential effect of isotope fractionation during chromatographic separation. Large Cr isotope fractionation was demonstrated during reduction of Cr(VI) to Cr(III) (Ellis et al., 2002), a process that is part of our anion exchange purification scheme. In analogy to the purification procedure used for natural samples described in Section 2.1, an aliquot of a Cr(VI) standard of known isotope composition (denoted as $\delta^{53/52}Cr_{standard}$; see Fig. 4) was loaded in dilute hydrochloric acid onto a chromatography column containing Dowex AG 1X8 anion resin. In contrast to the natural samples, this standard was not pre-spiked with the ^{50}Cr–^{54}Cr tracer. To investigate possible isotope fractionation during the reduction of Cr(VI) to Cr(III) additions of 2 mL 2 mol L^{-1} HNO_3 were repeatedly pipetted onto the resin over the course of several hours. The resulting elutions, containing partially reduced chromium, were collected in separate beakers. The chromium contents in these elutions were determined on small aliquots by ICP-OES and adequate amounts of the ^{50}Cr–^{54}Cr double spike were then added to the remaining elutions. After drying down the solutions the residues were taken up in 0.1 mol L^{-1} HNO_3 for mass spectrometric analyses.

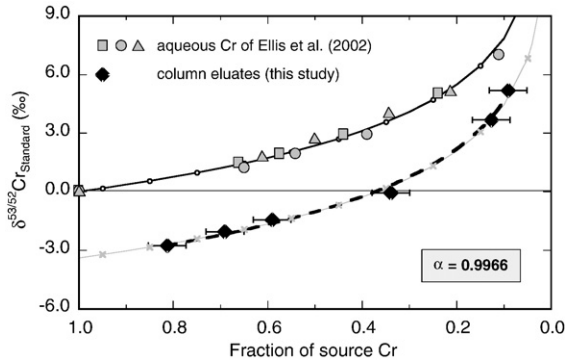

Fig. 4. Results from Cr(VI) reduction experiments: $\delta^{53/52}Cr$ values of supernate fractions from reduction experiments plotted as grey symbols (graphically rescaled data from Ellis et al. (2002) and $\delta^{53/52}Cr$ values of eluted chromium from column experiments plotted as filled diamonds (data from this study, see Table 1) as function of the remaining fraction of source chromium. The curves correspond to a Rayleigh fractionation with $\alpha = 0.9966$‰.

The double spike addition to the partial Cr elutions prior to mass spectrometric isotope analyses allows correction of the instruments mass bias. However, since the ^{50}Cr–^{54}Cr tracer was added to the elutions after chemical purification by anion exchange, the double spike correction does not account for any Cr isotope fractionation as a result of the chromatographic treatment. Indeed, when the Cr isotope compositions of the different elutions are plotted as function of the respective fraction of Cr(VI) that remained on the anion resin, the data follow a Rayleigh distillation function, perfectly reproducing the $10^3 \times \ln\alpha$ ($\approx \Delta^{53/52}Cr_{Cr(III)-Cr(VI)}$) of −3.4‰ previously determined by Ellis et al. (2002) (see Table 1; Fig. 4). This observation clearly demonstrates the need to account for unwanted Cr isotope fractionation by anion exchange. Such unwanted fractionation will most likely take place through incomplete reduction of Cr(VI) to Cr(III). However, addition of the ^{50}Cr–^{54}Cr double spike to the samples prior to chemical purification accounts for such effects. This is demonstrated by the Cr isotope data obtained for the NIST SRM 3112a standard (Table 1; Fig. 1) in a total of 15 sessions over the course of 22 months. As was already mentioned in Section 2.3.1, for each of these sessions an aliquot of our NIST SRM 3112a standard was spiked with the ^{50}Cr–^{54}Cr tracer and was then subjected to Cr purification by the anion exchange method, with a yield between 80 and 90%, prior to mass spectrometric analyses. The accuracy of the NIST SRM 3112a data (Fig. 1) clearly shows that our double spike method accounts for any isotope effects that may occur during the chemical purification of chromium.

3. Results and discussion

3.1. Silicate rocks

$\delta^{53/52}Cr_{SRM\ 979}$ values of seven mantle xenoliths range from −0.017 to −0.167‰ and those of ten ultramafic rocks and cumulates range from −0.009 to −0.211‰, respectively (Table 2, Fig. 5). Major element compositions for most of these samples can be found in Schoenberg and Blanckenburg (2006). Six oceanic and continental terrestrial basalts cover a very narrow range in Cr isotope compositions with $\delta^{53/52}Cr_{SRM\ 979}$ values between −0.126 and −0.178‰ with an average $\delta^{53/52}Cr_{SRM\ 979}$ value of −0.151±0.050‰ (2SD). $\delta^{53/52}Cr_{SRM\ 979}$ values for the two basaltic standard reference materials BHVO-1 and JB-1 yield slightly lighter isotope compositions than previously determined (Ellis et al., 2002), but both data sets reproduce within uncertainties (see Fig. 5). Unlike iron, for which a small isotopic contrast between mantle xenoliths and basalts was reported (Weyer et al., 2005; Schoenberg and Blanckenburg, 2006; Weyer and Ionov, 2007), chromium isotope compositions do not differ between basalts and mantle rocks. Although Cr-bearing mantle minerals (i.e. mainly spinel and clinopyroxene) contain chromium of the trivalent oxidation state, significant if not dominating amounts of Cr(II) have been reported by Berry et al. (2006) for basaltic melts, depending on the oxygen fugacity and the composition of the melt. Obviously, the contrasting oxidation states of chromium in mantle rocks and basaltic melts during partial mantle melting – be it of congruent or incongruent nature – does not cause Cr isotope fractionation. This is different from iron isotopes, for which a small difference in composition between mantle rocks and basalt was suggested to be the result of partial mantle melting (Weyer et al., 2005; Weyer and Ionov, 2007). The one granite sample GS-N that was analyzed in this study has an identical Cr isotope composition as the basalts and mantle rocks.

The homogenized top 25 cm of six sediment cores from the northeastern Arabian Sea have been determined for Cr isotope composition. These cores sample a variety of marine redox environments ranging from oxic to anoxic sediment conditions (Staubwasser and Sirocko, 2001). Anoxic sediment surface conditions are reached within the oxygen minimum zone of the water column between 200 and 1000 m depth. The $\delta^{53/52}Cr_{SRM\ 979}$ values of these sediments vary from +0.009 to −0.078‰, with an average value of −0.032±0.065‰. Student *t*-tests reveal that the difference of their mean $\delta^{53/52}Cr_{SRM\ 979}$ values to those of the mean igneous silicate Earth ($\delta^{53/52}Cr_{SRM\ 979}$ = −0.124±0.101‰) is significant. This small difference can be speculated to be due to three possible causes: (1) weathering or hydrothermal processes releasing preferentially heavy Cr into rivers; (2) a speciation change of dissolved Cr in seawater (Rue et al., 1997); (3) diagenetic processes altering the sediments' Cr isotope compositions, similar to the diagenetic Fe cycling observed in these sediments (Staubwasser et al., 2006).

3.2. Cr(III)-rich minerals

$\delta^{53/52}Cr_{SRM\ 979}$ values of chromite ($(Fe,Mg)Cr_2O_4$) separates from three lower group (LG-1, LG-3, and LG-5), one middle group (MG-3), and the two upper group (UG-1 and UG-2) chromitite layers of the western Bushveld Complex, South Africa, and from the chromitite seams 1, 2, 3, 6, 9, and 10 (top to bottom) of the Great Dyke, Zimbabwe, vary between −0.025 and −0.116‰ with an average $\delta^{53/52}Cr_{SRM\ 979}$ value of −0.082 ±0.058‰ (2 SD). Massive chromitite layers form when new ultramafic melt is injected into a magma chamber containing evolved, fractionated melt, driving the composition of the mixed, hybrid magma into the stability field of chromite (Irvine, 1977). Since the evolved magma is depleted in chromium, the crystallizing chromites reflect the isotope composition of the injected ultramafic melt and it is thus not surprising that the different chromites are indistinguishable in $\delta^{53/52}Cr_{SRM\ 979}$ values from those of mantle xenoliths and ultramafic rocks and cumulates (Table 2, Fig. 5).

Essentially all of the technical chromium that is used for industrial purposes is mined from prominent chromitite layers of layered igneous intrusions, amongst which the Bushveld Complex is the economically most important one. Significant Cr isotope fractionation during the extraction of chromium from the ore by smelting to form ferrochrome is very unlikely, since the smelting process operates at high temperatures (1600–1700 °C) and is very efficient. Oxidation of the extracted chromium to industrially utilizable "chemical-grade" Cr(VI) is also very efficient and significant Cr isotope fractionation therefore unlikely. Thus, the invariable $\delta^{53/52}Cr_{SRM\ 979}$ values of chromite ores are a good proxy for the Cr isotope

Table 2
Cr isotope compositions of silicate igneous rocks and sediments

Sample	Origin	Cr [μg g^{-1}]	±	2 SD [abs.]	$\delta^{53/52}Cr_{SRM\ 979}$	±	2 SD[a]	N
Mantle xenoliths								
CH70-5 (spinel-lherzolite)	Val Moleno, Swiss Alps	2103	±	11	−0.125	±	0.048	2
La-SJ/Per (spinel-lherzolite)	Salinas de Janubio, Lanzarote	4588	±	23	−0.151	±	0.068	3
MIH-Per/1 (spinel-lherzolite)	Finero, Italy	1381	±	7	−0.041	±	0.048	3
MIH-Per/2					−0.017	±	0.048	1
MIH-Per/4 (dunite)	locality unknown, New Zealand	5095	±	25	−0.115	±	0.048	3
GZG1275/3 (wherlite)	Odenwald, Germany	1361	±	7	−0.167	±	0.048	1
GZG1275/4 (harzburgite)	Harz mountains, Germany	2274	±	11	−0.111	±	0.066	2
		Mean mantle rocks			*−0.104*	±	*0.110*	*7*
Ultramafic rocks and cumulates								
Siss1 (gabbro)	Bergell Intrusion, Swiss Alps				−0.119	±	0.048	1
Siss4 (hbl-cumulate)	Bergell Intrusion, Swiss Alps				−0.048	±	0.048	1
Siss6 (hbl-cumulate)	Bergell Intrusion, Swiss Alps				−0.009	±	0.048	1
AK38	Akilia Island, Greenland				−0.161	±	0.048	1
AK05	Akilia Island, Greenland				−0.131	±	0.048	1
AK02	Akilia Island, Greenland				−0.139	±	0.048	1
GZG1275/5 (hornblendite)	Schriesheim, Germany	886.7	±	4.4	−0.133	±	0.048	1
GZG1275/6 (harzburgite)	Bushveld Complex, South Africa	2624	±	13	−0.101	±	0.105	2
GZG1275/7 (dunite)	Bushveld Complex, South Africa	2303	±	12	−0.211	±	0.048	2
GZG1275/8 (fayalite gabbro)	Harz mountains, Germany	134.3	±	0.7	−0.142	±	0.048	1
		Mean ultramafic cumulates			*−0.119*	±	*0.113*	*10*
Basalts								
BB-23 (in-house basalt)	Bramburg, Germany	256.2	±	1.3	−0.129	±	0.070	3
BE-N (CRPG basalt)	Essey-la-côte, France	298.1	±	1.5	−0.173	±	0.050	3
BHVO-1 (USGS basalt)	Hawaii, USA	244.3	±	1.2	−0.126	±	0.084	3
JB-1 (GSJ basalt)		394.0	±	2.0	−0.178	±	0.048	3
TUC (in-house basalt)	origin unknown	229.4	±	1.1	−0.129	±	0.048	3
OMAN (in-house basalt)	Semail Ophiolite, Oman	140.5	±	0.7	−0.171	±	0.100	2
		Mean basalts			*−0.151*	±	*0.050*	*6*
Others								
GS-N (USGS granite)	Vosges, France	42.51	±	0.21	−0.151	±	0.048	1
SDO-1 (USGS shale)	Ohio Shale, USA	53.78	±	0.27	−0.080	±	0.048	1
		Mean igneous silicate Earth			*−0.124*	±	*0.101*	*24*
Marine sediments								
1KG-12.5	Oxic	130.0	±	0.6	−0.016	±	0.048	1
87KG-12.5	Oxic	109.9	±	0.5	−0.053	±	0.048	1
183KG-12.5	Oxic	93.01	±	0.47	−0.007	±	0.048	1
173KG-12.5	Oxic (suboxic subsurface)	80.19	±	0.40	−0.045	±	0.048	1
155KG-12.5	Suboxic	118.3	±	0.6	−0.078	±	0.048	1
58KG-12.5	Suboxic (anoxic subsurface)	105.9	±	0.5	0.009	±	0.048	1
		Mean marine sediments			*−0.032*	±	*0.065*	*6*

CRPG = Centre de Recherches Pétrographiques et Géochimiques, Vandoeuvre lès-Nancy, France; USGS = United States Geological Survey, Denver, USA; GSJ = Geological Survey of Japan.
All Cr concentrations were determined by isotope dilution using double spike MC-ICP-MS.
[a] Uncertainties are given as calculated according to Eq. (5) or the 2SD of replicate measurements, whichever was larger.

composition of technical chromium. Nevertheless, the Cr isotope compositions of different purified Cr standard solutions with $\delta^{53/52}Cr_{SRM\ 979}$ values of −0.443 to +0.023‰ reported here (Table 1; Fig. 5), and various chemical reagents such as $K_2Cr_2O_7$ and $Cr(NO_3)^{2-}$ and chromic acid supplies used to make up plating baths with $\delta^{53/52}Cr_{SRM\ 979}$ values between −0.07 and +0.37‰ reported by (Ellis et al., 2002) slightly deviate from the Cr isotope compositions of chromite ores. The observed variations in the Cr isotope compositions of these chemical reagents may be due to the processes that were employed to further purify the chromium or, in the case of the plating baths, be the result of small Cr isotope fractionation through electro-plating (Ellis et al., 2002). Knowledge of the Cr isotope composition of technical chromium is insofar important, as it marks the initial isotope composition of the anthropogenic Cr(VI) pollutant. This in turn allows to determine the degree of natural attenuation of Cr(VI) in groundwater through its Cr isotope composition that fractionates along a Rayleigh distillation curve with ongoing reduction of Cr(VI) to Cr(III) in the aquifer (Blowes, 2002; Ellis et al., 2002).

Two fuchsites ($K(Al,Cr)_3Si_3O_{10}(OH)_2$) and two uvarovites ($Ca_3Cr_2(SiO_4)_3$) from different metamorphic belts around the

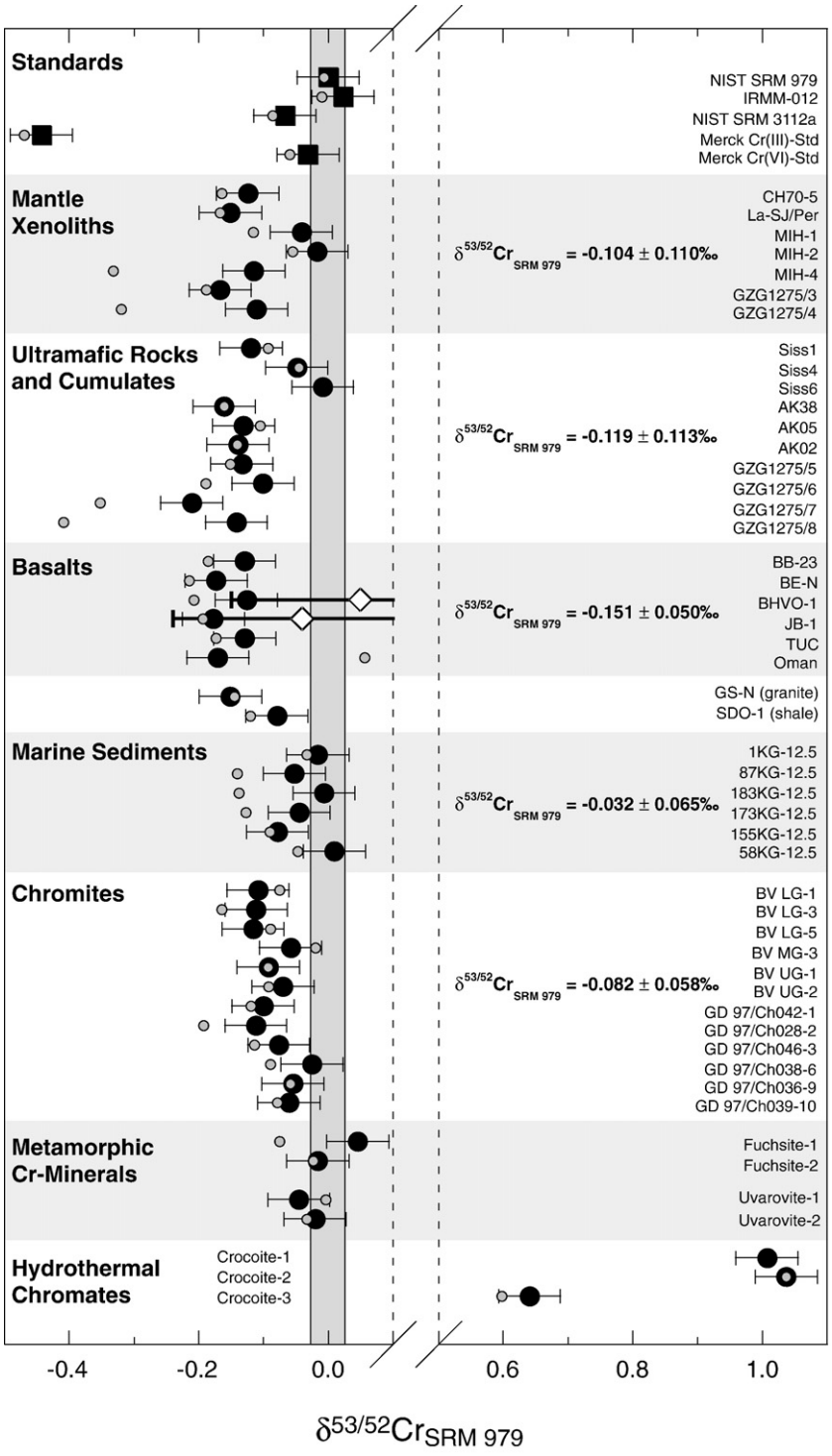

Fig. 5. $\delta^{53/52}Cr_{SRM\ 979}$ values of different chromium standard solutions (solid squares), silicate Earth reservoirs, marine sediments from the Arabian Sea and Cr-rich minerals (all as solid circles). Open diamonds give the $\delta^{53/52}Cr_{SRM\ 979}$ values of the BHVO-1 and JB-1 standard reference materials reported by Ellis et al. (2002) that are within uncertainties identical to our values. Small grey dots give the $\delta^{53/52}Cr_{SRM\ 979}$ values for the corresponding samples that were not corrected for the interferences of Ti, V, and Fe. Usually the difference between the interference-corrected and -uncorrected $\delta^{53/52}Cr_{SRM\ 979}$ values of a sample is less than 0.1‰, demonstrating the excellent chemical purification of chromium from these elements. The vertical shaded area gives the 2 standard deviation external reproducibility of chromium standard measurements (see Fig. 1b).

world have Cr isotope compositions between −0.046 and +0.046‰ in $\delta^{53/52}Cr_{SRM\ 979}$. Given the small number of samples it is impossible to assess whether the Cr isotope compositions of these minerals are statistically distinct from those of the igneous Earth. However, as a first qualitative observation it appears that metamorphic minerals (Table 3) show no or very little Cr isotope fractionation from their potential protolith rocks (Table 2).

Table 3
The Cr isotope composition of igneous, metamorphic, and hydrothermal Cr-minerals

Sample	Origin	$\delta^{53/52}Cr_{SRM\ 979}$	±	2 SD [a]	N
Chromites					
BV LG-1	Bushveld Intrusion, South Africa	−0.109	±	0.048	2
BV LG-3	Bushveld Intrusion, South Africa	−0.111	±	0.051	2
BV LG-5	Bushveld Intrusion, South Africa	−0.116	±	0.048	2
BV MG-3	Bushveld Intrusion, South Africa	−0.058	±	0.094	2
BV UG-1	Bushveld Intrusion, South Africa	−0.093	±	0.048	2
BV UG-2	Bushveld Intrusion, South Africa	−0.070	±	0.060	2
GD 97/Ch042-1	Great Dyke, Zimbabwe	−0.100	±	0.086	2
GD 97/Ch028-2	Great Dyke, Zimbabwe	−0.112	±	0.049	2
GD 97/Ch046-3	Great Dyke, Zimbabwe	−0.076	±	0.049	2
GD 97/Ch038-6	Great Dyke, Zimbabwe	−0.025	±	0.048	1
GD 97/Ch036-9	Great Dyke, Zimbabwe	−0.055	±	0.048	1
GD 97/Ch039-10	Great Dyke, Zimbabwe	−0.061	±	0.048	1
	Mean chromites	*−0.082*	±	*0.058*	
Metamorphic minerals					
Fuchsite-1	Maine, USA	0.046	±	0.048	1
Fuchsite-2	Norway	−0.016	±	0.048	1
Uvarovite-1	Biserski, Russia	−0.046	±	0.048	1
Uvarovite-2	Oxford, Canada	−0.020	±	0.048	1
Hydrothermal chromates					
Crocoite-1	Beresovsk, Russia	1.007	±	0.049	1
Crocoite-2	Yekaterinburg, Russia	1.037	±	0.049	1
Crocoite-3	Calenberg, Germany	0.640	±	0.048	1

[a] Uncertainties are given as calculated according to Eq. (5) or the 2SD of replicate measurements, whichever was larger.

3.3. Crocoites

The $\delta^{53/52}Cr_{SRM\ 979}$ values of three lead-chromate crocoite ($PbCrO_4$) samples determined in this study are 1.007‰ (Beresovsk, Russia), 1.037‰ (Yekaterinburg, Russia), and 0.640‰ (Calenberg, Germany). Crocoite forms as secondary phase in oxidizing domains of hydrothermal systems, when Cr-rich fluids released from ultramafic rocks – usually through serpentinization – penetrate through galena (PbS) or other lead-rich lithologies (Frost, 2004). Some of the cumulate rocks investigated in this study, though being partially serpentinized, still share a common Cr isotope composition with mantle xenoliths, as do metamorphic minerals (see 3.3.2.). It is therefore unlikely, that serpentinization or other processes that release chromium from ultramafic rocks into a passing fluid significantly fractionate Cr isotopes. There are several

Table 4
Cr isotope fractionation through crocoite precipitation

Sample	pH [a]	$f_{Cr(VI)}$ in solution	$\delta^{53/52}Cr_{SRM\ 979}$ solution	±	2 SD [b]	$\delta^{53/52}Cr_{SRM\ 979}$ crocoite	±	2 SD [b]	N
Crocoite precipitation experiment 1									
Prec1–1	7.01	1.00	−0.032	±	0.024				2
Prec1–2	6.14	0.75	−0.028	±	0.024	0.007	±	0.024	2
Prec1–3	2.94	0.50	−0.081	±	0.024	0.048	±	0.026	2
Prec1–4	2.32	0.34	−0.106	±	0.024	0.044	±	0.024	2
Prec1–5	1.94	0.18	−0.179	±	0.041	0.021	±	0.024	2
Prec1–6	1.60	0.08	−0.292	±	0.035	−0.005	±	0.024	2
Prec1–7	1.41	0.07	−0.358	±	0.038	0.012	±	0.037	2
Prec1–8	1.18	0.08	−0.428	±	0.024	0.017	±	0.024	2
Crocoite precipitation experiment 2									
Prec2–1	1.65	0.95	−0.008	±	0.025				3
Prec2–2	1.65	0.80	−0.039	±	0.064	0.044	±	0.024	3
Prec2–3	1.65	0.66	−0.032	±	0.035	0.009	±	0.042	3
Prec2–4	1.65	0.50	−0.040	±	0.077	−0.002	±	0.030	3
Prec2–5	1.65	0.08	−0.244	±	0.073	−0.008	±	0.048	3
Prec2–6	1.65	0.04	−0.385	±	0.105	−0.016	±	0.062	3

[a] Uncertainties of pH measurements are in the order of ±0.01.
[b] Uncertainties are given as calculated according to Eq. (5) – using the external reproducibility for standards (i.e. 0.024‰) instead of natural samples – or the 2SD of replicate measurements, whichever was larger.

possibilities that may explain the heavy Cr isotope compositions of crocoites; (1) Cr(III) in the fluid is partially oxidized to Cr (VI), which is accompanied by an enrichment in heavy Cr isotopes for the oxidized form. However, it has not yet been determined whether oxidation of Cr(III) to Cr(VI) is really accompanied by a mass-dependent fractionation of the Cr isotopes and thus for the moment an assessment of the feasibility for this scenario is impossible. (2) During percolation of the fluid through the rock, Cr(VI) in the fluid is partially reduced to Cr(III), a process during which the residual Cr(VI), from which the crocoites form, is enriched in heavy Cr isotopes (Ellis et al., 2002). (3) Transfer of Cr(VI) from the fluid into the crocoite crystal structure causes isotope fractionation through changes in the bonding environment of Cr. This hypothesis was tested by carrying out partial crocoite precipitation experiments.

In a first experiment variable amounts of a 1000 ppm lead solution in 0.5 mol L^{-1} HNO_3 were added to several centrifuge tubes containing 50 ppm CrO_4^{2-} in a phosphate buffer solution to precipitate variable amounts of $PbCrO_4$ at room temperature. With the use of the KH_2PO_4/Na_2HPO_4 buffer an adjustment of a pH of 7 for the mixed solutions was attempted. However, although precipitation of crocoite in this experiment was successful, the measured pH in the resulting mixtures decreased with the amount of lead solution added (see crocoite precipitation experiment 1 in Table 4), indicating that the capacity of the buffer solution was too low. To overcome this problem, a second set of experiments was carried out. This time a lead solution was prepared by dissolving a $Pb(NO_3)_2$ salt in purified H_2O to avoid additional protons from an acid solution. Again, different amounts of this lead solution were added to three sets of centrifuge tubes all containing a 50 ppm CrO_4^{2-} solution. However, the chromate in each of the three sets was taken up in a different buffer solution, attempted to maintain different pH levels; a pH of 6.5 with a KH_2PO_4/Na_2HPO_4 buffer, a pH of 3 with an HCl/Na-citrate buffer, and a pH of 1.65 with a HCl/KCl buffer. Lead and chromium contents of the precipitates were determined by ICP-OES. At pH = 6.5 stoichiometry of the precipitates corresponded to $Pb(NO_3)_2$, but not to $PbCrO_4$. Very little and irregular amounts of crocoite were precipitated at a pH of 3. Since the chromate solutions in the HCl/Na-citrate buffer lost their typical yellow color even before adding any lead, it is assumed that the citrate in the buffer solution (partially) reduced the CrO_4^{2-} to $Cr(OH)_2^+$ and $Cr(OH)_3$ that appear colorless at such low concentrations. None of the solutions or precipitates of the pH = 6.5 and pH = 3 sets of experiments were further investigated. At a pH of 1.65 crocoite precipitation was observed with a clear correlation between the amounts of lead added to the chromate solutions and precipitated $PbCrO_4$. The HCl/KCl buffer maintained a constant pH of 1.65 ± 0.01 for all lead:chromate mixtures of this set (see crocoite precipitation experiment 2 in Table 4). Crocoite precipitates and residual chromate solutions of the two successful precipitation experiments were separated by centrifugation and then treated like natural samples – i.e. addition of adequate amounts of double spike and Cr purification by anion exchange chromatography – before mass spectrometric analyses.

The Cr isotope results of the two experiments are reported in Table 4 and shown in Fig. 6. In both sets of experiments the crocoites are enriched in heavy Cr isotopes compared to the respective Cr(VI) solutions from which they precipitated. The data of both sets of experiments follow a Rayleigh distillation function with $10^3 \times \ln\alpha$ ($\approx \Delta^{53/52}Cr_{(crocoite-Cr(VI)aq)}$) of +0.10 ± 0.05‰ (Fig. 6). This implies that the crocoite precipitate as the reaction product is isolated from isotopic exchange with $CrO_4^{2-}{}_{(aq)}$, which is inconsistent with closed-system isotope equilibrium. It is difficult to assess the mode of fractionation that takes place during crocoite precipitation. A purely kinetic isotope fractionation between $CrO_4^{2-}{}_{(aq)}$ and crocoite can be excluded, because the reaction product would then be expected to be enriched in light and not heavy Cr isotopes. A large isotope effect between $CrO_4^{2-}{}_{(aq)}$ and crocoite is not expected anyway, because chromium is tetrahedrally coordinated by oxygen in both these compounds.

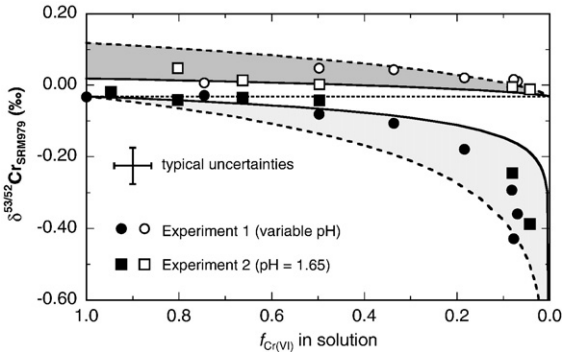

Fig. 6. $\delta^{53/52}Cr_{SRM\ 979}$ values of crocoite precipitates (open symbols) and CrO_4^{2-} in the residual solutions (solid symbols) versus the fraction of Cr remaining in the solutions. Rayleigh distillation curves with $\alpha = 1.00005$ (solid lines) and 1.00015 (stippled lines) are given for comparison.

Chromium isotope fractionation during crystallization of crocoite from hydrothermal fluids can be ruled out to explain the heavy Cr isotope compositions of up to 1.037‰ in $\delta^{53/52}Cr_{SRM\ 979}$ observed for natural crocoites, given the small isotope fractionation of +0.10 ± 0.05‰ at 20 °C. A single process as cause for these heavy isotope compositions of crocoites that crystallized from medium- to high-temperature hydrothermal environments also appears implausible, when considering theoretical predictions for chromium isotope fractionation (Schauble et al., 2004). Thus, the heavy Cr isotope composition of natural crocoites are most likely the result of isotope fractionation during hydrothermal Cr cycling involving repeated redox processes.

4. Conclusions

Double spike addition to samples before chemical purification of chromium eliminates the risk of undetectable artificial Cr isotope fractionation during Cr separation through ion exchange methods, while allowing for highly accurate and precise chromium isotope ratio measurements by high-resolution MC-ICP-MS. The external reproducibility of an in-house Cr standard solution was as good as 0.024‰ in $\delta^{53/52}Cr_{SRM\ 979}$. The external reproducibility on the $\delta^{53/52}Cr_{SRM\ 979}$ value of natural samples was calculated from replicate analyses of rocks and minerals and yielded a value of 0.048‰. Using this new technique the first important results are as follows.

1) The presented mantle xenoliths, ultramafic rocks and cumulates, as well as oceanic and continental basalts have identical chromium isotope compositions. Thus, the change in the preferred oxidation state of chromium from Cr(III) in solid mantle rocks to predominantly Cr(II) in the corresponding basaltic melts produced by partial mantle melting (Berry et al., 2006) appears not to cause measurable Cr isotope fractionation.

2) Chromite ores from prominent chromitite layers of layered igneous intrusions from the Bushveld Complex, South Africa and the Great Dyke, Zimbabwe contain Cr isotope ratios that are indistinguishable to those of the igneous silicate Earth. Since these deposits present also the major source of technical chromium used in metal plating, tanning, colour and other industries, this ratio presents a benchmark value against which sources of environmental Cr(VI) pollution can be compared. Knowledge of the original Cr isotope composition of a Cr(VI)-pollutant allows to model the efficiency of natural chromium attenuation in soils and aquifers.

3) Either weathering and/or transport processes, hydrothermal activity, a change in the speciation of Cr in seawater, or diagenetic Cr cycling appears to introduce a minor Cr isotope fractionation, as revealed by the slightly heavier Cr isotope composition of Arabian Sea sediments compared to igneous silicate rocks.

4) Natural crocoites show heavy Cr isotope compositions of up to 1.037‰ in $\delta^{53/52}Cr_{SRM\ 979}$. These significant isotope fractionations are likely due to redox processes during hydrothermal Cr cycling. Once the Cr isotope fractionation factors during oxidation and reduction at moderate to high temperatures are established, Cr isotope systematics bear the potential to serve as a tool to depict and quantify changes in the redox conditions along hydrothermal pathways.

Acknowledgements

We thank Monika Guelke for her help with microwave digestions and Alexandra Tangen for laboratory support. We are grateful to Robert Frei (Geological Institute, University of Copenhagen) for providing the enriched Cr isotope tracers from which our ^{50}Cr–^{54}Cr double spike was prepared. Tom Johnson is thanked for providing unpublished Cr isotope data of standards that allowed inter-laboratory comparison. Two anonymous reviewers and the editor Bernard Bourdon are thanked for detailed comments that helped to improve the quality of this work. Cytec Industries Incorporation is thanked for providing free samples of the liquid phosphine oxide Cyanex 923 for testing iron, titanium, and vanadium separation from chromium. This project was financially supported by German Research Foundation (DFG) grant SCHO1071/3-1 to RS.

References

Albarede, F., et al., 2004. Precise and accurate isotopic measurements using multiple-collector ICPMS. Geochimica Et Cosmochimica Acta 68 (12), 2725–2744.

Anbar, A.D., Roe, J.E., Barling, J., Nealson, K.H., 2000. Nonbiological fractionation of iron isotopes. Science 288, 126–128.

Arnold, G.L., Weyer, S., Anbar, A.D., 2004. Fe isotope variations in natural materials measured using high mass resolution multiple collector ICPMS. Analytical Chemistry 76 (2), 322–327.

Ball, J.W., Bassett, R.L., 2000. Ion exchange separation of chromium from natural water matrix for stable isotope mass spectrometric analysis. Chemical Geology 168 (1–2), 123–134.

Berry, A.J., Neill, H.S., Scott, D.R., Foran, G.J., Shelley, J.M.G., 2006. The effect of composition on Cr2+/Cr3+ in silicate melts. American Mineralogist 91 (11–12), 1901–1908.

Blowes, D., 2002. Environmental chemistry — tracking hexavalent Cr in groundwater. Science 295 (5562), 2024–2025.

Compston, W., Oversby, V.M., 1969. Lead isotopic analysis using a double spike. Journal of Geophysical Research 74 (17) 4338-&.

De Laeter, J.R., et al., 2003. Atomic weights of the elements: review 2000 — (IUPAC technical report). Pure and Applied Chemistry 75 (6), 683–800.

Dideriksen, K., Baker, J.A., Stipp, S.L.S., 2006. Iron isotopes in natural carbonate minerals determined by MC-ICP-MS with a Fe-58–Fe-54 double spike. Geochimica Et Cosmochimica Acta 70 (1), 118–132.

Ellis, A.S., Johnson, T.M., Bullen, T.D., 2002. Chromium isotopes and the fate of hexavalent chromium in the environment. Science 295 (5562), 2060–2062.

Ellis, A.S., Johnson, T.M., Bullen, T.D., 2004. Using chromium stable isotope ratios to quantify Cr(VI) reduction: lack of sorption effects. Environmental Science & Technology 38 (13), 3604–3607.

Frei, R., Rosing, M.T., 2005. Search for traces of the late heavy bombardment on Earth — results from high precision chromium isotopes. Earth and Planetary Science Letters 236 (1–2), 28–40.

Frost, R.L., 2004. Raman microscopy of selected chromate minerals. Journal of Raman Spectroscopy 35 (2), 153–158.

Götz, A., Heumann, K.G., 1988. Chromium trace determination in inorganic, organic and aqueous samples with isotope-dilution mass-spectrometry. Fresenius Zeitschrift Fur Analytische Chemie 331 (2), 123–128.

Irvine, T.N., 1977. Origin of chromitite layers in Muskox intrusion and other stratiform intrusions — new interpretation. Geology 5 (5), 273–277.

Johnson, C.M., Beard, B.L., 1999. Correction of instrumentally produced mass fractionation during isotopic analysis of Fe by thermal ionization mass spectrometry. International Journal of Mass Spectrometry 193, 87–99.

Johnson, C.M., Beard, B.L., Albarède, F. (Eds.), 2004. Geochemistry of Non-traditional Stable Isotopes. Reviews in Mineralogy and Geochemistry, vol. 55. Mineralogical Society of America, Blacksburg.

Lugmair, G.W., Shukolyukov, A., 1998. Early solar system timescales according to Mn-53–Cr-53 systematics. Geochimica Et Cosmochimica Acta 62 (16), 2863–2886.

Maréchal, C.N., Télouk, P., Albarède, F., 1999. Precise analysis of copper and zinc isotopic compositions by plasma-source mass spectrometry. Chemical Geology 156, 251–273.

Remya, P.N., Reddy, M.L., 2004. Solvent extraction separation of titanium(IV) vanadium(V) and iron(III) from simulated waste chloride liquors of titanium minerals processing industry by the trialkyphosphine oxide Cyanex 923. Journal of Chemical Technology and Biotechnology 79 (7), 734–741.

Rue, E.L., Smith, G.J., Cutter, G.A., Bruland, K.W., 1997. The response of trace element redox couples to suboxic conditions in the water column. Deep-Sea Research Part I — Oceanographic Research Papers 44 (1), 113–134.

Schauble, E., Rossman, G.R., Taylor, H.P., 2004. Theoretical estimates of equilibrium chromium-isotope fractionations. Chemical Geology 205 (1–2), 99–114.

Schoenberg, R., Blanckenburg, F.v., 2006. Modes of planetary-scale Fe isotope fractionation. Earth and Planetary Science Letters 252 (3–4), 342–359.

Schoenberg, R., von Blanckenburg, F., 2005. An assessment of the accuracy of stable Fe isotope ratio measurements on samples with organic and inorganic matrices by high-resolution multicollector ICP-MS. International Journal of Mass Spectrometry 242 (2–3), 257–272.

Shields, W.R., Murphy, T.J., Catanzar, Ej, Garner, E.L., 1966. Absolute isotopic abundance ratios and atomic weight of a reference sample of chromium. Journal of Research of the National Bureau of Standards Section a — Physics and Chemistry, A 70 (2) 193-&.

Siebert, C., Nägler, T.F., Kramers, J.D., 2001. Determination of molybdenum isotope fractionation by double spike multicollector inductively coupled

plasma mass spectrometry. Geochemistry, Geophysics, Geosystems 2 2000GC000124.

Staubwasser, M., Sirocko, F., 2001. On the formation of laminated sediments on the continental margin off Pakistan: the effects of sediment provenance and sediment redistribution. Marine Geology 172 (1–2), 43–56.

Staubwasser, M., von Blanckenburg, F., Schoenberg, R., 2006. Iron isotopes in the early marine diagenetic iron cycle. Geology 34 (8), 629–632.

Weyer, S., Ionov, D.A., 2007. Partial melting and melt percolation in the mantle: the message from Fe isotopes. Earth and Planetary Science Letters 259 (1–2), 119–133.

Weyer, S., Schwieters, J., 2003. High precision Fe isotope measurements with high mass resolution MC-ICPMS. International Journal of Mass Spectrometry 226, 355–368.

Weyer, S., et al., 2005. Iron isotope fractionation during planetary differentiation. Earth and Planetary Science Letters 240 (2), 251–264.

Young, E.D., Galy, A., Nagahara, H., 2002. Kinetic and equilibrium mass-dependent isotope fractionation laws in nature and their geochemical and cosmochemical significance. Geochimica Et Cosmochimica Acta 66 (6), 1095–1104.